lubricants

MDPI

Article

Small Laser-Textured Dimples for Improved Tribological Performance of CoCrMo in Artificial Hip Joints

William B. Bennett [1,2] and Min Zou [1,2,*]

[1] Department of Mechanical Engineering, University of Arkansas, Fayetteville, AR 72701, USA; wbennett@uark.edu
[2] Center for Advanced Surface Engineering, University of Arkansas, Fayetteville, AR 72701, USA
* Correspondence: mzou@uark.edu; Tel.: +1-479-575-6671

Abstract: This study investigates the impact of small dimples on the tribological properties of CoCrMo (CCM) surfaces. Laser-ablated textures with 5 μm diameter dimples were fabricated at varying aspect ratios (0.1, 0.2, 0.3) and surface densities (5%, 15%, 25%) to evaluate their effects on friction and wear when paired with ultra-high molecular weight polyethylene (UHMWPE) counterfaces. The results showed that small dimples significantly reduced and stabilized the coefficient of friction (CoF) and wear compared to untextured CCM and larger dimples as reported in the literature. The texture configuration with a 5% surface density and 0.1 aspect ratio achieved the best combination of friction and wear performance by facilitating the formation of a stable and uniform lubricant film during sliding. These findings underscore the potential of small, precisely engineered surface textures to improve the tribological performance of CCM, offering a promising approach for reducing friction and wear in artificial hip joints.

Keywords: small dimples; laser surface texturing; CoCrMo; artificial hip joint; surface engineering; friction and wear performance

check for updates

Received: 21 February 2025
Revised: 22 March 2025
Accepted: 27 March 2025
Published: 2 April 2025

Citation: Bennett, W.B.; Zou, M. Small Laser-Textured Dimples for Improved Tribological Performance of CoCrMo in Artificial Hip Joints. *Lubricants* **2025**, *13*, 158. https://doi.org/10.3390/lubricants13040158

Copyright: © 2025 by the authors. Licensee MDPI, Basel, Switzerland. This article is an open access article distributed under the terms and conditions of the Creative Commons Attribution (CC BY) license (https://creativecommons.org/licenses/by/4.0/).

1. Introduction

Total hip replacement (THR) surgery has significantly improved quality of life for individuals suffering from severe arthritis or joint injuries. In 2021 alone, over 450,000 THR procedures were performed in the United States, and the number is expected to rise with the aging population [1]. Despite their success, the longevity of artificial hip joints remains a critical concern, as wear-induced implant failure is one of the primary reasons for revision surgeries [2]. The articulation between the femoral head and acetabular liner generates wear particles that may lead to osteolysis, ultimately necessitating revision surgery [3,4].

To address wear-related challenges, extensive research has explored strategies to reduce friction and wear in metal-on-polyethylene (MoP) hip implants. Approaches such as low-friction surface coatings [5,6], cross-linked polyethylene liners [7,8], and surface texturing of CoCrMo (CCM) femoral heads have been investigated. Among these, surface texturing has emerged as a promising technique due to its ability to enhance lubrication, reduce contact stress, and improve load distribution. Textured dimples serve as lubricant reservoirs, reducing direct asperity contact and improving tribological performance [9–11].

Artificial hip joints operate under dynamic loading conditions, where lubrication transitions among boundary, mixed, and elasto-hydrodynamic (EHL) regimes depending on motion, contact pressure, and lubricant properties. Textured surfaces influence these lubrication transitions by promoting fluid retention and pressure redistribution, improving load-carrying capacity in orthopedic applications [12,13]. Optimized textures can extend the

duration of EHL lubrication, preventing lubricant starvation and reducing wear-induced damage [14,15].

Laser surface texturing (LST) offers a precise, repeatable method to fabricate micro- and nano-scale textures on CCM surfaces [16–18]. Prior studies have shown that textured CoCrMo surfaces with dimples (~100 µm) improve wear resistance and reduce friction in hip implants [19]. Chyr et al. [20] demonstrated that a 5% surface density of 100 µm diameter dimples lowered the coefficient of friction (CoF) from 0.26 to 0.12 under a maximum contact pressure of 0.57 MPa. However, at higher contact pressures (1.13 MPa), untextured surfaces outperformed all textured samples, as the microtextures failed to generate sufficient load-carrying capacity to support the increased load and reduce friction. These findings emphasize the importance of tailoring texture designs for specific operating conditions.

The performance of dimpled textures depends on parameters such as diameter, depth, and surface density [21]. Langhorn et al. [22] reported a 68% wear reduction using 100 µm diameter dimples with an optimal aspect ratio of 0.01 (1 µm depth) and 10% surface density on CCM. Despite these findings, most existing studies focus on large dimples (≥20 µm diameter) and exhibit significant wear after extended testing, often without detailed friction data to clarify wear mechanisms [23].

Small dimples (~5 µm in diameter) offer a biomimetic advantage, closely resembling the smallest natural features of human cartilage [24]. The higher dimple density associated with smaller dimples allows for improved lubricant retention, better hydrodynamic lift, and enhanced load distribution. For example, at 25% surface density, the 300 mm^2 contact area in a hip joint can accommodate 15.3 million 5 µm diameter dimples—44 times more than the 38,000 dimples possible with a 100 µm diameter (Figure 1) [25]. This increased density reduces the spacing between dimples, ensuring consistent lubricant reservoirs and superior tribological performance.

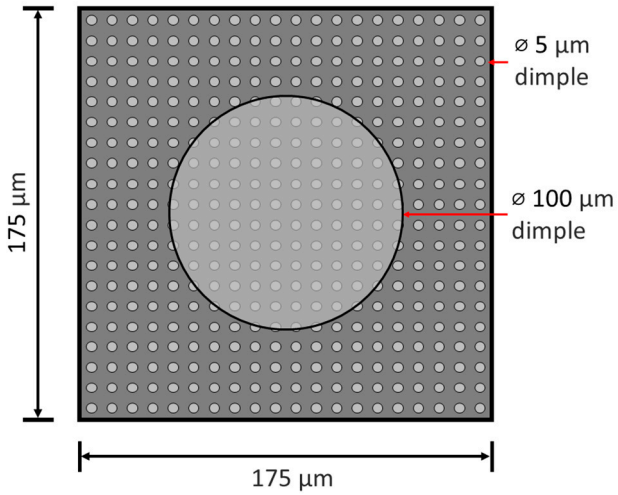


Figure 1. At a 25% surface texture density, a 175 µm × 175 µm area can accommodate only a single 100 µm diameter dimple, but can fit up to 400 dimples with a diameter of 5 µm.

Despite their potential, small dimples fabricated via laser ablation have rarely been studied in tribological research for artificial hip joints. This study investigates how varying aspect ratios and surface densities of 5 µm diameter dimples affect the friction and wear performance of CCM femoral heads. The tribological properties of textured samples are compared against those of untextured CCM to quantify the advantages of small dimple textures. By demonstrating that small dimples outperform the untextured surfaces and

larger dimples reported in the literature, this study aims to extend the lifespan of MoP artificial hip joints and improve the quality of life for THR recipients.

2. Experimental Methods

2.1. Sample Fabrication

In this study, ASTM F1537 CoCrMo (CCM) discs, supplied by United Performance Metals (Cincinnati, OH, USA), were tested against ultra-high molecular weight polyethylene (UHMWPE) pins made from GUR1020-E, a highly cross-linked material treated with 100 kGy of radiation and stabilized with vitamin E (VEHXL) from Orthoplastics (Bacup, UK). CCM was selected due to its high mechanical strength, exceptional corrosion resistance, and biocompatibility, making it a preferred material for artificial hip joints [1]. UHMWPE was chosen as the counterface material for its proven performance in metal-on-polyethylene (MoP) configurations, offering excellent biocompatibility, durability, and chemical inertness [26].

The CCM discs were fabricated from a 12.7 mm diameter rod and machined into discs approximately 1.5 mm thick. These discs were polished in several stages to achieve a mirror finish and flatness on both sides. The polishing process began with coarse polishing under a 10 lb load using 1200-grit sandpaper for two 50 s intervals. This was followed by intermediate polishing for three minutes using a 6 µm polycrystalline diamond suspension, and a final polishing step using a 0.06 µm amorphous colloidal silica suspension for 90 s. During polishing, the specimen holder rotated at 60 rpm, while the polishing wheels operated at 150 rpm. After polishing, the discs were cleaned by submerging them in acetone and placing them in a 10 min sonication bath (Branson CPX2800, Branson Ultrasonics, Brookfield, CT, USA). They were then rinsed with isopropyl alcohol (IPA) and deionized (DI) water and dried with nitrogen gas.

Laser surface texturing (LST) was used to enhance the tribological performance of the CCM discs. Textures were created using a femtosecond laser machining system (Oxford Laser A5 Femtosecond, Oxford Lasers Ltd., Didcot, UK), which employed an Ytterbium-doped Potassium Gadolinium Tungstate (Yb:KGW) femtosecond laser with a wavelength of 532 nm, a pulse duration of less than 290 fs, and a maximum power output of 2.6 W. Grid patterns of circular dimples (Table 1) were fabricated using varying laser parameters, resulting in dimple diameters of 5 µm and depths of 0.5, 1.0, and 1.5 µm. These laser parameters, shown in Table 2, were chosen because they yielded the highest quality and most consistent dimples across textures. Surface densities of 5%, 15%, and 25% were achieved by adjusting the spacing between laser pulses. A dwell time of 0.1 s was applied between each pulse to ensure uniformity in dimple shape and depth. The texture density and depth ranges were selected to encompass the optimal values identified in the literature [20,22].

Table 1. Design characteristics of various laser-textured samples.

Texture Type	Diameter (µm)	Depth (µm)	Aspect Ratio	Surface Density (%)
A1	5	0.5	0.1	5
A2	5	1.0	0.2	5
A3	5	1.5	0.3	5
B1	5	0.5	0.1	15
B2	5	1.0	0.2	15
B3	5	1.5	0.3	15
C1	5	0.5	0.1	25
C2	5	1.0	0.2	25
C3	5	1.5	0.3	25

Table 2. Laser parameters for fabricating dimples with different aspect ratios.

Aspect Ratio	Power (%)	Drill Time (s)	RA Divider	Frequency (Hz)
0.1	15	0.08	800	700
0.2	20	0.10	800	700
0.3	22	0.15	800	700

The VEHXL UHMWPE pins were machined from a 40 mm diameter, 500 mm long rod into individual pins measuring 4 mm in diameter and 12 mm in length using a CNC machine (PCNC 440, Tormach, Madison, WI, USA). The machining process included an initial leveling step to flatten the bulk material, followed by precise fabrication of the pins to their target dimensions. A small notch was drilled into each pin edge to serve as a reference point. Prior to testing, the pins were cleaned thoroughly with IPA and DI water and dried using nitrogen gas to ensure surface cleanliness.

2.2. Surface Topography Characterization

The surface topography of the fabricated CCM discs and VEHXL UHMWPE pins was characterized using a 3D laser scanning confocal microscope (LSCM, VK-X260, Keyence Corporation, Itasca, IL, USA). To ensure reliable and reproducible results, three scans were conducted for each sample. Key parameters, including dimple depth profiles, average surface roughness (Sa), and root mean square surface roughness (Sq), were measured and analyzed. Standard deviations were calculated to provide a comprehensive assessment of the surface texture and its consistency.

2.3. Water Contact Angle Measurements

Water contact angle (WCA) measurements were conducted using a goniometer (OCA 15, DataPhysics Instruments, Charlotte, NC, USA) to assess the wettability of both textured and untextured samples. Prior to measurement, the samples were cleaned by submerging them in acetone, followed by a 10 min sonication bath. After rinsing with DI water, the samples were dried using nitrogen gas. A 3 µL droplet of DI water was carefully deposited onto the sample surface using a syringe, and a backlit image of the droplet was captured. The left and right contact angles were measured and averaged to determine the WCA. For consistency, three measurements were performed for each sample.

2.4. Pin-on-Disc Tribological Testing

Tribological testing was conducted using a pin-on-disc setup with a tribometer (UMT-2, Bruker, San Jose, CA, USA), as shown in Figure 2. To simulate the lubricating environment of a natural hip joint, a mixture of 25% bovine calf serum (BCS, Sigma-Aldrich, St. Louis, MO, USA) and 75% DI water was used as the lubricant. The lubricant temperature was maintained at 37 °C to replicate physiological conditions. A VEHXL UHMWPE pin, measuring 4 mm in diameter, was positioned to slide against a CCM disc in an oscillating motion along a circular arc. The tribometer applied a normal load of 15 N, with the pin oscillating at a frequency of 1 Hz within a 30-degree arc, positioned 4 mm from the disc center. The sliding speed was set at 1 mm/s, and the test was conducted for a total duration of eight hours. These parameters were chosen to best mimic the dynamic motion and contact mechanics of a hip joint during walking, where the femoral head undergoes an arcuate motion against the acetabular cup, rather than a purely linear reciprocating motion. The CoF was calculated as the ratio of the measured friction force to the applied normal load, providing reliable data on the tribological performance of the samples.

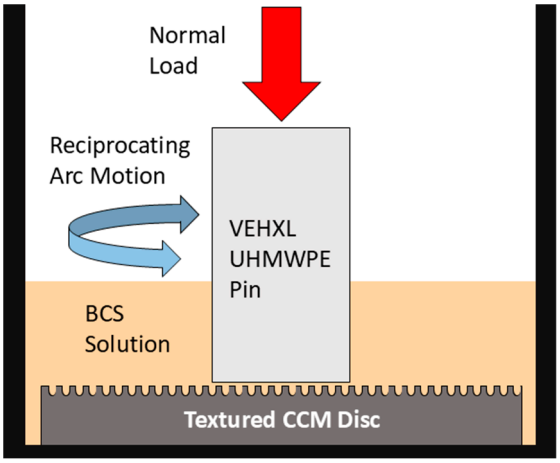


Figure 2. Pin-on-disc experimental setup, showing a VEHXL UHMWPE pin pressed against a textured CoCrMo (CCM) sample submerged in bovine calf serum (BCS) and kept at 37 °C (not to scale).

2.5. Wear Analysis

Wear analysis was performed based on the wear track on the CCM discs and changes in the surface roughness of the VEHXL UHMWPE. High-resolution imaging of the wear tracks was conducted using scanning electron microscopy (SEM) and 3D LSCM to visualize the wear patterns and transfer films. Changes in the surface roughness of the VEHXL UHMWPE pins were analyzed by generating 3D surface maps using LSCM. The pre- and post-test roughness values (Sa) were calculated, and the differences were used to assess the extent of pin wear.

3. Results

3.1. Surface Topography of Fabricated CCM Disc and UHMWPE Pin

The sample surfaces were analyzed at 20× magnification using 3D LSCM. The arrays of dimples for all textured samples are shown in Figure 3. Different surface densities result in varying numbers of dimples within the same area by altering their pitch. Specifically, at 5% surface density, 12 dimples are observed, while 48 and 88 dimples are present at 15% and 25% surface densities, respectively. Textures with lower aspect ratios display a lighter interior surrounded by a darker heat-affected zone around the edges of the dimples.

Figure 4 illustrates the cross-sectional profiles of dimples with three different aspect ratios at a 5% surface density. The femtosecond laser used for fabrication achieved precise dimple depths with excellent dimensional accuracy, even at microscale feature sizes. However, slight protrusions, rising above the surface, sporadically appear on the perimeters of some dimples. These protrusions may contribute to the generation of wear debris during extended rubbing.

The average surface roughness (Sa) and root mean square roughness (Sq) of the textured CCM discs are plotted in Figure 5. As expected, all textured samples exhibit higher roughness values compared to the untextured sample. In general, textures with higher surface densities show greater roughness, while aspect ratio has a much smaller impact on the roughness of the samples. However, as surface density increases, and more dimples contribute to the surface topography, aspect ratio has a greater effect on surface roughness.

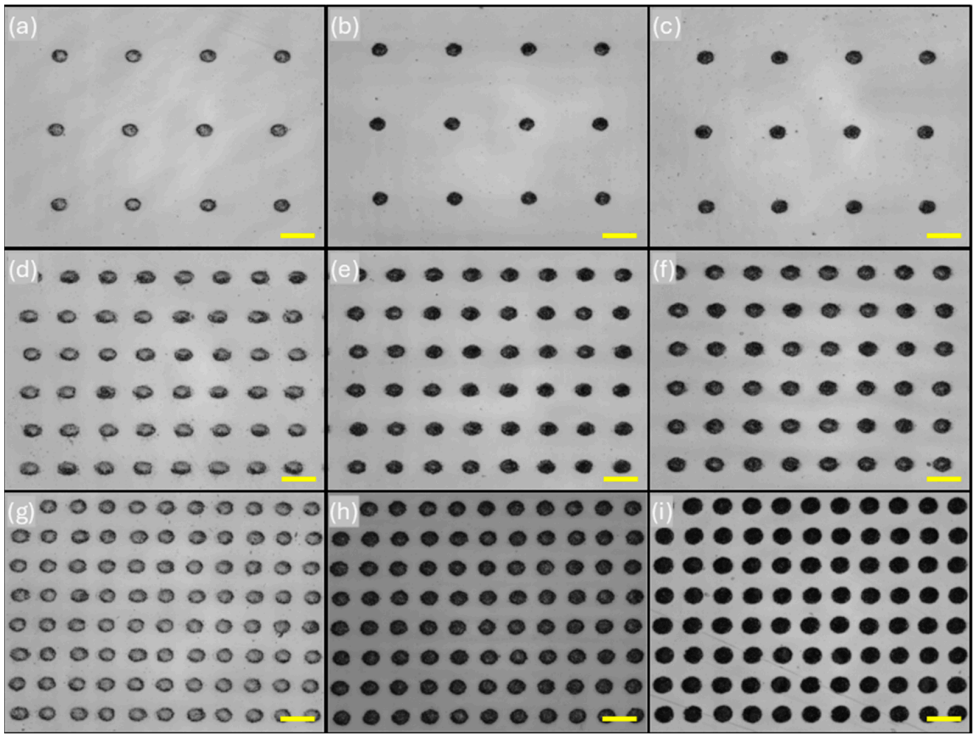


Figure 3. LSCM images of all surface textures: (**a**) A1, (**b**) A2, (**c**) A3, (**d**) B1, (**e**) B2, (**f**) B3, (**g**) C1, (**h**) C2, and (**i**) C3 (all scale bars are 10 μm).

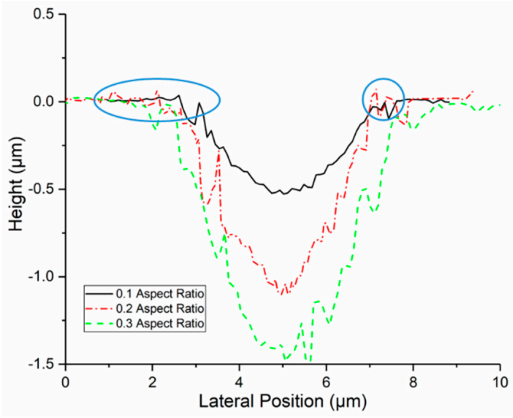


Figure 4. Cross-sectional profiles of dimples at different aspect ratios of 5% surface density textures. Protrusions around the edge have been circled.

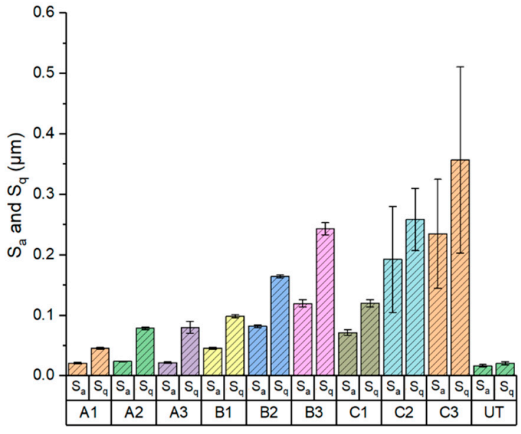


Figure 5. The average surface roughness, S_a, and root mean square roughness, S_q, of different CCM textures.

For the VEHXL UHMWPE pins, the CNC machining process produced a grooved surface texture, as shown in Figure 6. The R_a and R_q of the pins were measured at 2.168 µm and 2.612 µm, respectively. These grooves closely resemble the texture and roughness of new UHMWPE cups used in artificial hip replacements. For instance, Choudhury et al. reported an R_a value of 1.96 µm for a brand new UHMWPE cup [27].

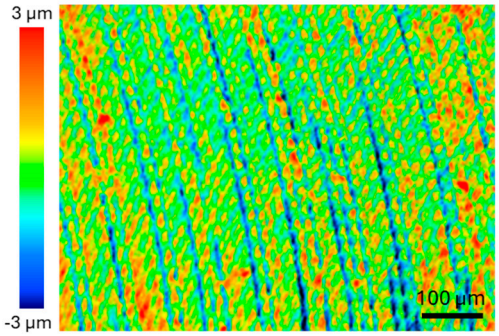


Figure 6. Surface finish of CNC-fabricated VEHXL UHMWPE pin showing machining grooves like new artificial cups.

3.2. Surface Wettability

The WCAs for the nine laser-textured surfaces and the untextured CCM sample, as shown in Figure 7, reveal significant differences in surface wettability. The untextured CCM sample exhibited slight hydrophobicity, with a mean WCA of 91.8°. In contrast, all laser-textured surfaces consistently displayed hydrophilic behavior. Among the textured samples, Texture C3 was the least hydrophilic, with a mean WCA of 84.9°, while Texture A2 demonstrated the highest hydrophilicity, achieving a mean WCA of 62.4°. Surface density was identified as the most influential factor, with textures at 5% density exhibiting the lowest WCAs and strongest hydrophilicity. Aspect ratio, on the other hand, had no significant impact on surface wettability.

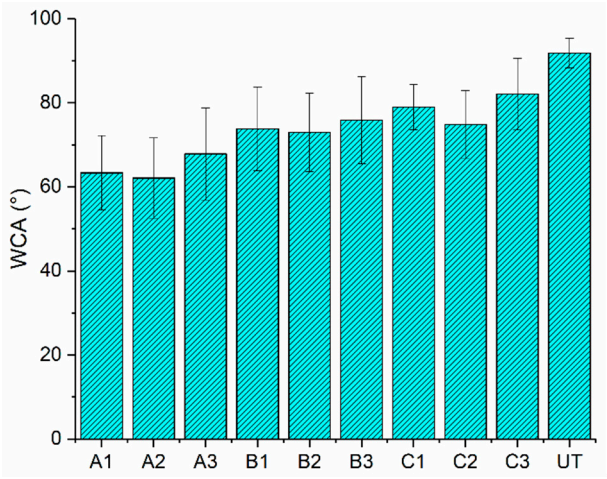


Figure 7. Water contact angles of different textures on CCM.

The reduction in WCA due to laser texturing can be attributed to changes in both surface chemistry and geometry. Laser texturing modifies the oxide layer, leading to changes in surface energy and wettability. While metals generally have higher surface free energy than their oxides, the passive oxide layer on CoCrMo plays a critical role in wetting behavior. Laser processing promotes the growth and restructuring of chromium oxide, which can enhance hydrophilicity depending on its thickness, composition, and nanostructuring. Additionally, the geometric features of the surface influence wetting

behavior through the Wenzel [28] and Cassie–Baxter models [29]. For example, textures such as A1 and A2 (5% density, aspect ratios 0.1 and 0.2) achieved the lowest WCAs (62–70°), consistent with the Wenzel model, where water fully penetrates the surface features, increasing the effective solid–liquid contact area. In contrast, denser textures, such as C3 (25% density, aspect ratio 0.3), exhibited higher WCAs (~85°) due to the Cassie–Baxter model, where air pockets trapped within the texture reduce the effective contact area. Despite this, Texture C3 still showed a lower WCA than the untextured surface, underscoring the effects of laser-induced oxide modification and topographical changes on wettability.

Overall, the data in Figure 7 highlight that both oxidation-induced hydrophilicity and texture geometry work synergistically to enhance surface wettability. Sparse, shallow textures like A1 and A2 maximize water spreading due to high hydrophilicity, while denser, deeper textures like C3 retain moderate hydrophilicity. This enhanced hydrophilicity is particularly advantageous for self-lubrication in joint applications, as it helps retain lubricants on the textured surfaces, reducing friction and improving tribological performance.

3.3. Friction and Wear Performance

3.3.1. Coefficient of Friction

Tribological tests were conducted on CCM with VEHXL UHMWPE as the counterface material, and the average CoF results are shown in Figure 8. All laser-textured samples exhibited lower CoF values compared to untextured CCM, with the lowest CoF reaching just 60% of the untextured sample. This underscores the effectiveness of laser texturing in enhancing tribological performance.

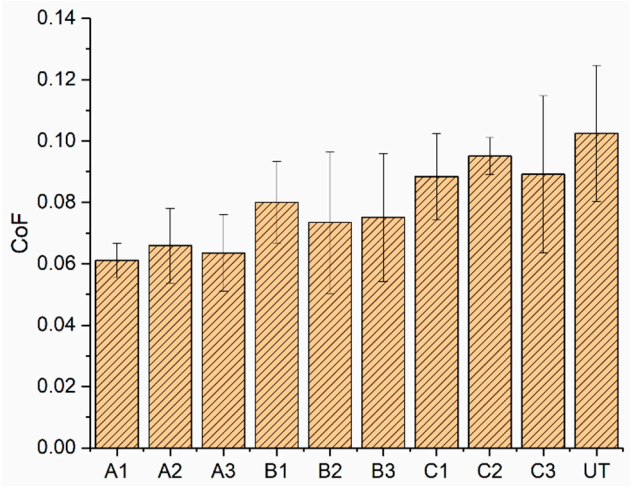


Figure 8. Coefficient of friction values of different dimple textures.

Among the factors studied, surface density emerged as the most influential in reducing CoF. Textures with a 5% surface density achieved the lowest CoF values, outperforming those with higher surface densities. A clear trend was observed: as surface density increased, CoF values rose, which aligns with the trend observed in WCA data. These findings highlight a strong correlation between surface hydrophilicity and reduced CoF.

In contrast, the aspect ratio exhibited a much weaker and inconsistent effect on CoF, which suggests that the aspect ratio may play a less significant role in the performance of small diameter dimples, where the dominant factors are likely the overall density and ability to promote lubricant retention. Notably, the lowest CoF value recorded in this study demonstrated a friction reduction, from 15% to 50%, compared to the lowest CoF values reported in the literature for textured CCM under similar testing conditions [30,31], further

highlighting the effectiveness of small-diameter dimples when paired with optimized surface density.

These results further emphasize the potential of laser texturing, particularly through optimizing surface density, to significantly improve the friction performance of CCM in tribological applications.

3.3.2. Frictional Behavior

The representative CoF plots in Figure 9 reveal that all laser-textured samples exhibit lower and more stable friction compared to untextured CCM. While the untextured samples displayed substantial fluctuations in CoF throughout the eight-hour tests, the textured surfaces maintained consistent and steady values. This stability is likely due to the enhanced ability of textured surfaces to retain and support the formation of a stable lubricant film. In contrast, untextured surfaces are less effective at maintaining lubricant coverage, leading to intermittent lubricant loss and sharp increases in CoF.

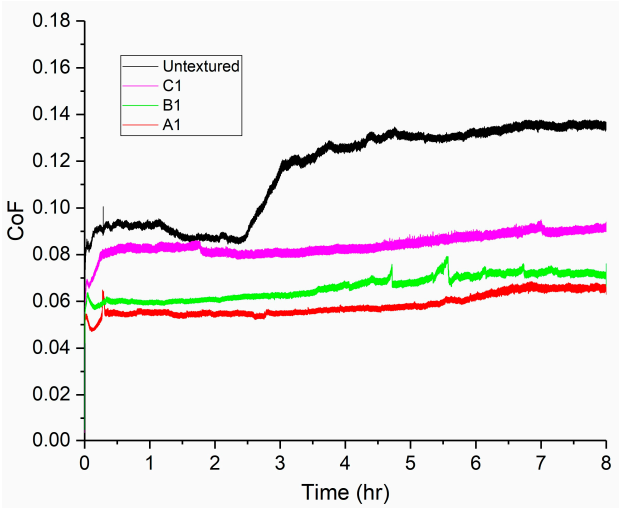


Figure 9. Coefficients of friction for representative textured CCM samples compared to an untextured sample, tested against a VEHXL UHMWPE pin.

Among the textured samples, Texture A1 achieved the lowest CoF, with an average reduction of approximately 40% compared to the untextured samples. This remarkable improvement highlights the effectiveness of laser texturing in not only reducing friction, but also providing a more reliable and consistent tribological performance. These findings emphasize the critical role of laser texturing in optimizing frictional behavior, particularly by promoting stable lubrication and reducing frictional resistance.

3.3.3. Wear Performance and Mechanisms

Figure 10 presents SEM and LSCM images of the CCM wear tracks and dimples within the wear track after testing, along with transfer film thickness measurements. The LSCM images (Figure 10c,d) correlate closely with the SEM images of the same region (Figure 10a,b), showing that the darker regions in the SEM images correspond to areas with thicker transfer films from the VEHXL UHMWPE pin. In these regions, the transfer film thickness reaches up to 109 nm, as measured in Figure 10e. Conversely, the lighter areas on the wear tracks exhibit little to no measurable transfer film, indicating minimal material transfer from the pin and negligible wear on the CCM surface. These findings highlight the localized nature of material transfer during testing, where thicker, more uniform transfer films are associated with increased surface interactions and higher CoFs.

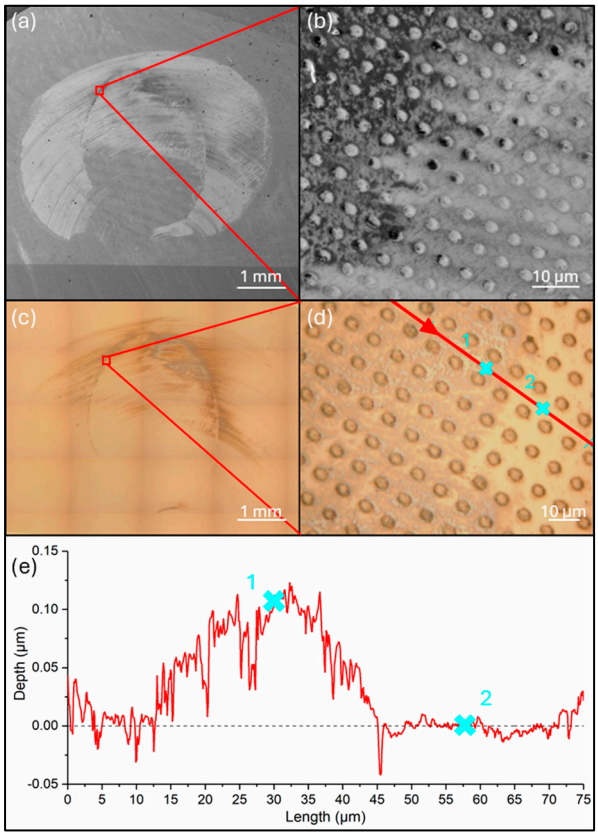


Figure 10. SEM images of a C1 sample after tribological testing: (**a**) wear track on the CCM surface and (**b**) magnified view of the dimples within the boxed region in (**a**). Corresponding optical image show (**c**) the wear track and (**d**) a magnified view of the dimples within the boxed region in (**c**). (**e**) Thickness profile of the transfer film along the red line in (**d**), with positions 1 and 2 labeled in cyan for reference.

Most CCM wear tracks showed no detectable wear. However, some samples exhibited 1–5 minor visible scratches, with depths reaching up to 108 nm (Figure 11). These scratches were observed near the transfer film areas, even when no visible wear was present on other areas of the wear track. These scratches corresponded to more severe wear on the VEHXL UHMWPE counterface pin. Given that VEHXL UHMWPE is significantly softer than the CCM disc, it is unlikely that the pin itself caused these scratches. Instead, the scratches are likely due to abrasive particles dislodged from the protruding rims around the edges of the laser-ablated dimples, as circled in the dimple profiles in Figure 4.

Out of nine tests conducted for each surface density, scratches were observed in two tests with 5% surface density, three tests with 15% surface density, and four tests with 25% surface density. This trend indicates that textures with higher surface densities are more prone to scratches on their wear tracks. The increased susceptibility to scratches is attributed to the greater number of dimples in higher density textures, which leads to more protrusions and, consequently, a higher likelihood of abrasive damage.

These protrusions form during laser ablation when certain regions of the CCM surface are insufficiently heated for complete material removal. Instead, these areas undergo a phase change that alters their surface topography, creating small, irregular protrusions. These protrusions are likely oxidized, making them harder, yet more brittle, than the surrounding material. During sliding, these protrusions can detach and act as abrasive debris, leading to three-body wear and causing the observed scratches on the CCM surface. The presence of these scratches correlated with a higher CoF and more significant transfer film, indicating higher wear.

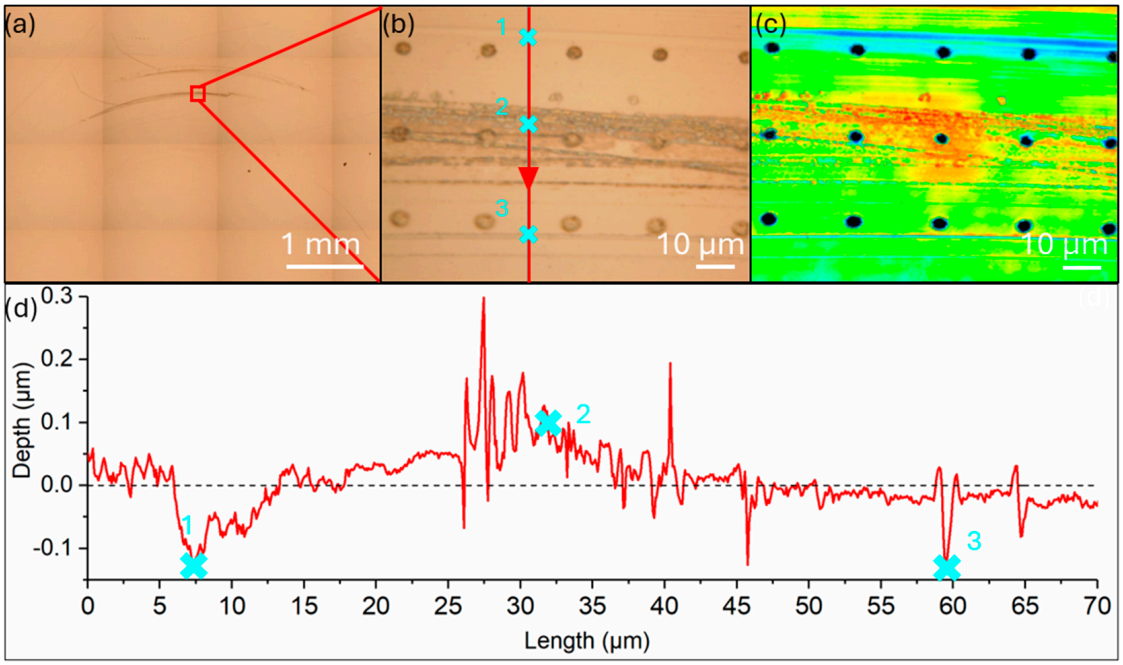


Figure 11. Scratches on an A1 sample after tribological testing: (**a**) optical image of the full wear track; (**b**) magnified optical image of a scratch and transfer film within the boxed region in (**a**); (**c**) height map corresponding to the close-up in (**b**); and (**d**) topographical line profile extracted along the red line in (**b**), showing scratch depths at positions 1 and 3, and the presence of transfer film at position 2.

The findings underscore the detrimental effects of these protrusions on the tribological performance of textured surfaces. The increased frequency of scratches in textures with higher surface densities further highlights the need to optimize laser processing parameters to minimize protrusion formation. By reducing these defects, the durability and tribological performance of laser-textured surfaces can be significantly improved.

The wear of the VEHXL UHMWPE pin was minimal, rendering it impractical to measure wear weight by comparing the pin's weight before and after testing. Instead, an indirect method was used to assess wear by evaluating changes in the pin's surface roughness. The initial surface of the pins displayed grooves resulting from the CNC machining process, as shown in Figure 6. After testing, surface roughness measurements conducted using LSCM revealed a reduction in these grooves, indicating wear (Figure 12). By comparing Figure 12b with Figure 12a, and Figure 12d with Figure 12c, reductions in height around the edges and the centers of the pins can be clearly observed.

Figure 13 illustrates the average surface roughness changes in the VEHXL UHMWPE pins for different textures. Among the 27 textured CCM samples, 19 showed smaller roughness changes compared to the untextured samples, indicating reduced pin wear when paired with laser-textured surfaces; in contrast, the remaining 8 samples exhibited larger roughness changes, primarily due to significant scratches on the VEHXL UHMWPE pin surface after testing. The variations in roughness changes within each sample group were largely driven by differing levels of scratches caused by individual samples within each group. Some samples, however, showed uncharacteristically low changes in roughness when compared to other tests on the same texture. For example, test #2 on texture C2 showed a 98% decrease in friction when compared to the average untextured test. This is due to its lower frequency of protrusions after fabrication, and more localized wear on the pin surface.

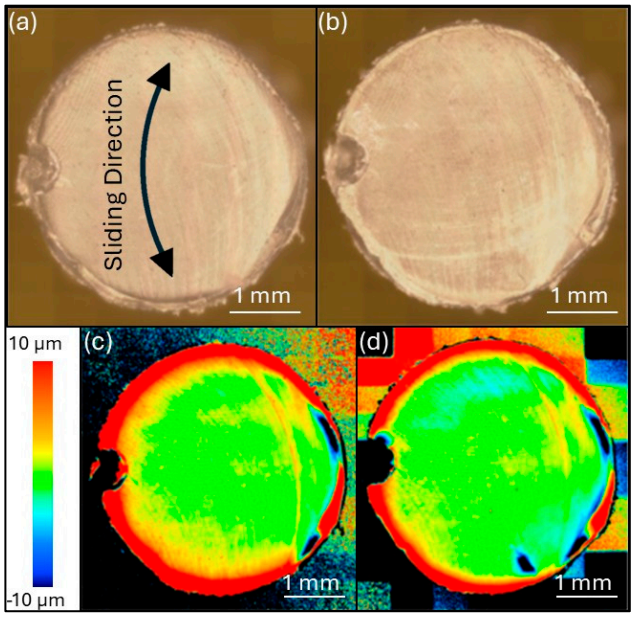


Figure 12. LSCM images of VEHXL UHMWPE pin surface (**a**,**c**) before and (**b**,**d**) after tribological testing.

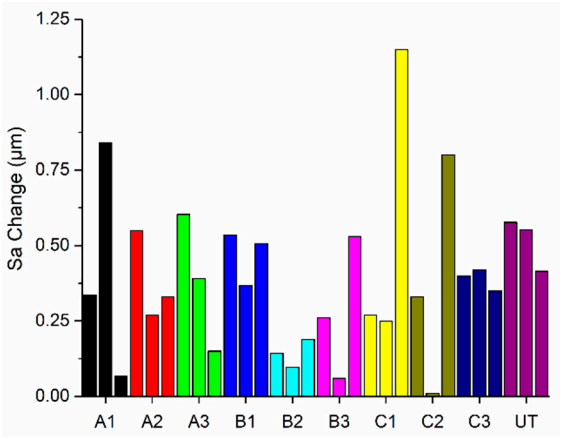


Figure 13. Average surface roughness changes in VEHXL UHMWPE pin after rubbing against different CCM textures.

4. Discussion

4.1. Wear

Quantifying wear in this study was challenging due to the shorter test duration compared to longer studies that use simpler methods, such as measuring pin weight loss [20,22] or wear track dimensions [32]. Despite this limitation, minimal wear was observed on the CCM surface, highlighting the durability and longevity of laser-textured surfaces. In contrast, wear primarily occurred on the VEHXL UHMWPE pins, as evidenced by the smoothing of their surfaces and the presence of transfer films on the CCM. Studies under similar conditions showed measurable wear on the UHMWPE pins despite fewer testing cycles [31], and/or showed lesser differences in wear when compared to an untextured sample [33]. These small-dimpled textures showed overall improvement in wear when compared to an untextured CCM sample.

Larger areas of wear tracks, marked by thicker transfer films on the CCM surface, indicate greater material transfer from the pin to the disc, signifying higher wear rates. Similarly, the significant reduction in the height of grooves on the VEHXL UHMWPE pins after testing reflects increased pin wear. This reduction in grooves on the pin surface, combined

with LSCM imaging confirming transfer film on the surface on the CCM, indicates that the transfer film is from the wear on the pin, not from the CCM itself.

Smaller CCM wear tracks, minimal changes in VEHXL UHMWPE pin surface roughness, and thinner transfer films on the CCM wear tracks served as clear indicators of reduced wear rates. These results underscore the critical importance of optimizing surface texture design to minimize wear and improve the tribological performance of CCM-VEHXL UHMWPE pairings.

4.2. Effect of Protrusions on Texture Performance

A side effect of LST was the formation of protruding rings around the dimple edges. These protrusions formed when regions of the CCM surface, insufficiently heated for complete ablation, underwent phase changes that altered the surface topography. Han et al. [34] reported a similar phenomenon, where pronounced and evenly distributed protrusions enhanced friction and wear performance by contributing to consistent surface interactions.

In this study, however, the protrusions were sporadic, shorter, and sharper, likely due to the lower laser power and shorter drill times used to create smaller dimples. Textures with lower aspect ratios were exposed to faster laser pulses, which further reduced the formation of protrusions. Unlike Han et al.'s study, the inconsistent and sharp protrusions in this work may have increased resistance during sliding, negatively impacting both friction and wear performance.

During testing, these protrusions often wore off and, in some cases, became trapped between the surfaces, leading to three-body wear and causing visible scratches on the CCM surface. Figure 11 highlights scratches as deep as 100 nm adjacent to transfer film marks, indicating higher wear in regions with scratches. This underscores the detrimental effects of irregular protrusions on tribological performance, emphasizing the need to optimize laser processing parameters to minimize their formation. Post-fabrication polishing steps were performed in an attempt to remove these protrusions and minimize their impacts on friction and wear performance. However, due to their small size and localized nature, effective removal proved challenging. Gentle polishing was insufficient to eliminate them, while more aggressive polishing unevenly altered the aspect ratio of the dimples across the texture, introducing additional variability in tribological performance.

4.3. Effect of WCA and Roughness on Tribological Performance

The formation of a stable and consistent lubricant film, which separates asperities between the two surfaces under lubricated conditions, is a key advantage of surface texturing. As shown in Figures 7 and 8, the trends in average WCA and CoF values suggest a correlation between increased wettability and improved tribological performance. Textures with lower average CoF values likely benefit from enhanced hydrophilicity, which promotes better lubricant retention. In addition to acting as lubricant reservoirs and enhancing hydrodynamic pressure, small dimples appear to increase the surface's affinity for lubricant, particularly at lower surface densities, where the Wenzel model dominates. This greater hydrophilicity facilitates the formation of a more stable lubricant film, thereby improving tribological properties.

In contrast, surface roughness played a less significant role in the tribological performance of the textures compared to WCA. At lower surface densities, the presence of small dimples did not substantially alter roughness compared to untextured CCM samples. However, at higher surface densities, an increased number of dimples led to a greater presence of protrusions, which had a stronger impact on tribological behavior than roughness alone. Comparing the CoF trends in Figure 8 with the roughness values in Figure 6, no

clear correlation emerges, especially when accounting for variations in aspect ratio. These findings suggest that wettability, rather than roughness, is the dominant factor influencing friction and wear in our study.

4.4. Mechanisms Governing Tribological Performance

The tribological improvements observed in this study are attributed to several interconnected mechanisms. Dimples function as lubricant reservoirs, enhancing the retention and distribution of bovine calf serum lubricant. This effect is particularly crucial in artificial hip joints, where lubrication shifts among boundary, mixed, and EHL regimes. In mixed lubrication, dimples provide micro-reservoirs that sustain lubrication film thickness, preventing dry contact and reducing wear. Under EHL, the localized pressure differentials around dimples generate hydrodynamic lift, facilitating stable lubricant film formation and minimizing direct asperity interactions.

Furthermore, surface texturing redistributes contact stresses, reducing peak contact pressures and mitigating material loss. This is particularly important under high-load conditions, where lubricant depletion can lead to increased friction and wear on untextured surfaces. Dimples also act as debris traps, capturing wear particles that would otherwise contribute to third-body abrasion, thereby extending implant longevity.

The effectiveness of these mechanisms is highly dependent on dimple geometry. The optimal texture identified in this study (5% surface density, 0.1 aspect ratio) demonstrated the lowest friction and wear due to a balance among effective lubricant retention, load distribution, and hydrodynamic enhancement. The findings underscore the critical role of surface texturing in regulating tribological behavior and enhancing the performance of metal-on-polyethylene hip implants.

5. Conclusions

This study demonstrates that LST is a highly effective method for fabricating precise sub-10 micron surface textures on CCM surfaces, significantly improving tribological performance. Small dimples with a 5 μm diameter were shown to reduce friction and wear effectively, making them well-suited for application in artificial hip joints.

Among the configurations tested, the texture design featuring a 5% surface density and a 0.1 aspect ratio was the most effective. This configuration achieved the lowest CoF and favorable wear rates, underscoring the critical role of optimizing texture geometry and density. The presence of dimples facilitated the formation of a stable and uniform lubricant film during sliding, which reduced asperity contact, lowered friction, and enabled consistent tribological performance.

However, this study also identified challenges associated with the laser texturing process. Sporadic protrusions formed around the edges of the dimples due to incomplete ablation, which negatively impacted performance by introducing irregular resistance and contributing to three-body wear. These protrusions caused visible scratches on the CCM surface and localized increases in wear, highlighting the importance of refining laser processing parameters to minimize their formation.

In summary, this work highlights the potential of LST to enhance the performance and longevity of artificial hip joints by improving lubrication and minimizing wear through precisely engineered surface textures. The findings provide valuable insights for optimizing texture designs and laser processing techniques, paving the way for more durable and efficient medical implants.

Future studies on small-dimpled textures should explore the effects of further reducing dimple diameter and adjusting key parameters, such as surface density, to optimize tribological performance. Given that the lowest coefficient of friction (CoF) was observed at

the lowest tested surface density (5%), additional experiments should investigate whether even lower surface densities could yield further reductions in CoF. Additionally, research should focus on mitigating the formation of protrusions, either by refining laser processing parameters or introducing a post-processing step before testing, to minimize their impact on wear behavior.

Author Contributions: Conceptualization, W.B.B. and M.Z.; methodology, W.B.B.; software, W.B.B.; validation, W.B.B.; formal analysis, W.B.B. and M.Z.; investigation, W.B.B.; resources, M.Z.; data curation, W.B.B.; writing—original draft preparation, W.B.B.; writing—review and editing, M.Z.; visualization, W.B.B.; supervision, M.Z.; project administration, M.Z.; funding acquisition, M.Z. All authors have read and agreed to the published version of the manuscript.

Funding: This research was funded by the University of Arkansas and the US National Science Foundation under Grant Award #OIA-1457888. Any opinions, findings, and conclusions or recommendations expressed in this material are those of the authors and do not necessarily reflect the views of the US National Science Foundation.

Data Availability Statement: The data used in this study are available upon reasonable request from the corresponding author.

Acknowledgments: We thank Orthoplastics for generously providing the VEHXL UHMWPE pins used in this study.

Conflicts of Interest: The authors declare that they have no known competing financial interests or personal relationships that could have appeared to influence the work reported in this paper.

Abbreviations

The following abbreviations are used in this manuscript:

CCM	CoCrMo
UHMWPE	Ultra-high molecular weight polyethylene
CoF	Coefficient of friction
THR	Total hip replacement
LST	Laser surface texturing
MoP	Metal-on-polyethylene
VEHXL	Vitamin E-stabilized highly cross-linked
IPA	Isopropyl alcohol
DI water	Deionized water
LSCM	Laser scanning confocal microscopy
WCA	Water contact angle
BCS	Bovine calf serum
SEM	Scanning electron microscopy

References

1. El-Desouky, I.I.; Helal, A.H.; Mansour, A.M.R. Ten-Year Survival of Ceramic-on-Ceramic Total Hip Arthroplasty in Patients Younger than 60 Years: A Systematic Review and Meta-Analysis. *J. Orthop. Surg. Res.* **2021**, *16*, 679. [CrossRef] [PubMed]
2. Nebergall, A.K.; Greene, M.E.; Laursen, M.B.; Nielsen, P.T.; Malchau, H.; Troelsen, A. 2017, Vitamin E Diffused Highly Cross-Linked Polyethylene in Total Hip Arthroplasty at Five Years. *Bone Jt. J.* **2017**, *99*, 577–584. [CrossRef]
3. Nakanishi, Y.; Nakashima, Y.; Fujiwara, Y.; Komohara, Y.; Takeya, M.; Miura, H.; Higaki, H. Influence of Surface Profile of Co-28Cr-6Mo Alloy on Wear Behaviour of Ultra-High Molecular Weight Polyethylene Used in Artificial Joint. *Tribol. Int.* **2018**, *118*, 538–546. [CrossRef]
4. Saleh, K.J.; Thongtrangan, I.; Schwarz, E.M. Osteolysis: Medical and surgical approaches. *Clin. Orthop. Relat. Res.* **2004**, *427*, 138–147. [PubMed]
5. Ching, H.A.; Choudhury, D.; Nine, M.J.; Abu Osman, N.A. Effects of Surface Coating on Reducing Friction and Wear of Orthopaedic Implants. *Sci. Technol. Adv. Mater.* **2014**, *15*, 014402. [CrossRef]

6. Kalayarasan, M.; Prabhu Raja, V.; Nithin, V.; Vivinkumar, S.; Vishwaanth, M. Comparative Study of Wear Behavior of Multilayer Coatings for Human Hip Prosthesis. *Appl. Mech. Mater.* **2015**, *787*, 528–533. [CrossRef]
7. Moro, T.; Kawaguchi, H.; Ishihara, K.; Kyomoto, M.; Karita, T.; Ito, H.; Nakamura, K.; Takatori, Y. Wear Resistance of Artificial Hip Joints with Poly(2-Methacryloyloxyethyl Phosphorylcholine) Grafted Polyethylene: Comparisons with the Effect of Polyethylene Cross-Linking and Ceramic Femoral Heads. *Biomaterials* **2009**, *30*, 2995–3001. [CrossRef]
8. Lestari, W.D.; Nugroho, A.; Ismail, R.; Jamari, J.; Bayuseno, A.P. Study of Wear Performance of Crosslinking UHMWPE Acetabular Liner for Artificial Hip Joint Made from CNC Milling. *IOP Conf. Ser. Mater. Sci. Eng.* **2021**, *1078*, 012009. [CrossRef]
9. López-Cervantes, A.; Domínguez-López, I.; Barceinas-Sánchez, J.D.O.; García-García, A.L. Effects of Surface Texturing on the Performance of Biocompatible UHMWPE as a Bearing Material during in Vitro Lubricated Sliding/Rolling Motion. *J. Mech. Behav. Biomed. Mater.* **2013**, *20*, 45–53. [CrossRef]
10. Zhao, C.; Jia, X.; Zhao, Q.; Ma, H.; Yu, Z.; Zhang, Z.; Du, W.; Zhang, H. Research Progress on the Effect of Surface Texture on the Friction Properties of CoCrMo Alloys. *Compos. Interfaces* **2024**, *31*, 1269–1290. [CrossRef]
11. Hidayat, T.; Jamari, J.; Bayuseno, A.P.; Ismail, R.; Tauviqirrahman, M.; Wijaya, P.N. Study of Lubrication Fluid Pressure in Artificial Hip Joint During Bowing (Ruku'). In *Lecture Notes in Mechanical Engineering, Proceedings of the 7th International Conference and Exhibition on Sustainable Energy and Advanced Materials (ICE-SEAM 2021), Melaka, Malaysia, 1 July 2022*; Springer: Singapore, 2022; pp. 303–306. [CrossRef]
12. Gao, L.; Yang, P.; Dymond, I.; Fisher, J.; Jin, Z. Effect of Surface Texturing on the Electrohydrodynamic Lubrication Analysis of Metal-on-Metal Hip Implants. *Tribol. Int.* **2010**, *43*, 1851–1860. [CrossRef]
13. Ranuša, M.; Odehnal, L.; Kučera, O.; Nečas, D.; Hartl, M.; Křupka, I.; Vrbka, M. Effect of Surface Texturing on Friction and Lubrication of Ti6Al4V Biomaterials for Joint Implants. *Tribol. Lett.* **2015**, *73*, 15. [CrossRef]
14. Shinkarenko, A.; Kligerman, Y.; Etsion, I. The Effect of Surface Texturing in Soft Elasto-Hydrodynamic Lubrication. *Tribol. Int.* **2009**, *42*, 284–292. [CrossRef]
15. Uddin, M.S.; Ibatan, T.; Shankar, S. Influence of Surface Texture Shape, Geometry and Orientation on Hydrodynamic Lubrication Performance of Plane-to-Plane Slider Surfaces. *Lubr. Sci.* **2016**, *29*, 153–181. [CrossRef]
16. Drescher, P.; Oldorf, P.; Dreier, T.; Schnell, G.; Peters, R.; Seitz, H. Ring-Shaped Surface Microstructures for Improved Lubrication Performance of Joint Prostheses. *Lubricants* **2020**, *8*, 45. [CrossRef]
17. Tarabolsi, M.; Klassen, T.; Mantwill, F.; Gärtner, F.; Siegel, F.; Schulz, A. Patterned CoCrMo and Al2O3 Surfaces for Reduced Free Wear Debris in Artificial Joint Arthroplasty. *J. Biomed. Mater. Res.* **2013**, *101*, 3447–3456. [CrossRef]
18. Mao, B.; Siddaiah, A.; Liao, Y.; Menezes, P.L. Laser Surface Texturing and Related Techniques for Enhancing Tribological Performance of Engineering Materials: A Review. *J. Manuf. Process.* **2020**, *53*, 153–173. [CrossRef]
19. Liu, Y.; Zhu, Q.; Wang, C.; Li, J. Tribological Behavior of CoCrMo Artificial Knee Joint with Symmetrically Biomimetic Textured Surfaces on PEEK. *Opt. Laser Technol.* **2023**, *157*, 108774. [CrossRef]
20. Chyr, A.; Qiu, M.; Speltz, J.W.; Jacobsen, R.L.; Sanders, A.P.; Raeymaekers, B. A Patterned Microtexture to Reduce Friction and Increase Longevity of Prosthetic Hip Joints. *Wear* **2014**, *315*, 51–57. [PubMed]
21. Chen, K.; Tang, Y. Research Progress on the Design of Surface Texture in Tribological Applications: A Mini-Review. *Symmetry* **2024**, *16*, 1523. [CrossRef]
22. Langhorn, J.; Borjali, A.; Hippensteel, E.; Nelson, W.; Raeymaekers, B. Microtextured CoCrMo Alloy for Use in Metal-on-Polyethylene Prosthetic Joint Bearings: Multi-Directional Wear and Corrosion Measurements. *Tribol. Int.* **2018**, *124*, 178–183. [CrossRef] [PubMed]
23. Allen, Q.; Raeymaekers, B. Surface Texturing of Prosthetic Hip Implant Bearing Surfaces: A Review. *J. Tribol.* **2020**, *143*, 040801. [CrossRef]
24. Longmore, R.B.; Gardner, D.L. The surface structure of ageing human articular cartilage: A study by reflected light interference microscopy (RLIM). *J. Anat.* **1978**, *126 Pt 2*, 353–365. [PubMed] [PubMed Central]
25. Hidayat, T.; Ammarullah, M.I.; Saputra, E.; Lamura, M.D.P.; KN, C.; Ismail, R.; Bayuseno, A.P.; Jamari, J. A Method for Estimating the Contact Area of a Dual-Mobility Total Hip Prosthesis. *AIP Adv.* **2024**, *14*, 015317. [CrossRef]
26. Puccio, F.D. Biotribology of Artificial Hip Joints. *World J. Orthop.* **2015**, *6*, 77–94. [CrossRef]
27. Choudhury, D.; Ranuša, M.; Fleming, R.A.; Vrbka, M.; Křupka, I.; Teeter, M.G.; Goss, J.; Zou, M. Mechanical Wear and Oxidative Degradation Analysis of Retrieved Ultra High Molecular Weight Polyethylene Acetabular Cups. *J. Mech. Behav. Biomed. Mater.* **2018**, *79*, 314–323. [CrossRef]
28. Wenzel, R.N. Resistance of Solid Surfaces to Wetting by Water. *Ind. Eng. Chem.* **1936**, *28*, 988–994. [CrossRef]
29. Cassie, A.B.D.; Baxter, S. Wettability of Porous Surfaces. *Trans. Faraday Soc.* **1944**, *40*, 546–551. [CrossRef]
30. Shen, G.; Zhang, J.; Fang, F. Study on the Effect of Hydrodynamic Pressure on the Tribological Performance of Textured Bioimplants. *Proc. Inst. Mech. Eng. Part C J. Mech. Eng. Sci.* **2021**, *236*, 3135–3145. [CrossRef]

31. Alvarez-Vera, M.; Ortega, J.A.; Ortega-Ramos, I.A.; Hdz-García, H.M.; Muñoz-Arroyo, R.; Díaz-Guillén, J.C.; Acevedo-Dávila, J.L.; Hernández-Rodriguez, M.A.L. Tribological and Microstructural Characterization of Laser Microtextured CoCr Alloy Tested against UHMWPE for Biomedical Applications. *Wear* **2021**, *477*, 203819. [CrossRef]
32. Yuan, S.; Lin, N.; Wang, W.; Zhang, H.; Liu, Z.; Yu, Y.; Zeng, Q.; Wu, Y. Correlation between surface textural parameter and tribological behaviour of four metal materials with laser surface texturing (LST). *Appl. Surf. Sci.* **2022**, *583*, 152410. [CrossRef]
33. Borjali, A.; Langhorn, J.; Monson, K.; Raeymaekers, B. Using a Patterned Microtexture to Reduce Polyethylene Wear in Metal-on-Polyethylene Prosthetic Bearing Couples. *Wear* **2017**, *392–393*, 77–83. [CrossRef]
34. Han, Y.; Liu, F.; Zhang, K.; Huang, Q.; Guo, X.; Wang, C. A Study on Tribological Properties of Textured Co-Cr-Mo Alloy for Artificial Hip Joints. *Int. J. Refract. Met. Hard Mater.* **2021**, *95*, 105463. [CrossRef]

Disclaimer/Publisher's Note: The statements, opinions and data contained in all publications are solely those of the individual author(s) and contributor(s) and not of MDPI and/or the editor(s). MDPI and/or the editor(s) disclaim responsibility for any injury to people or property resulting from any ideas, methods, instructions or products referred to in the content.